RNA BIOLOGY
2020, VOL. 17, NO. 2, 176–187
https://doi.org/10.1080/15476286.2019.1672514

Taylor & Francis
Taylor & Francis Group

RESEARCH PAPER

Mechanism for coordinate regulation of *rpoS* by sRNA-sRNA interaction in *Escherichia coli*

Wonkyong Kim and Younghoon Lee

Department of Chemistry, KAIST, Daejeon, Korea

ABSTRACT
RpoS is a key regulator of general stress responses in *Escherichia coli*. Its expression is post-transcriptionally up-regulated by the small RNAs (sRNAs), ArcZ, DsrA and RprA, through sRNA-*rpoS* mRNA interactions. Although overexpression of the sRNA, CyaR, was reported to down-regulate *rpoS* expression, how CyaR regulates *rpoS* has not been determined. Here, we report that CyaR represses *rpoS* expression by base-pairing with a region next to the ArcZ binding site in the 5′ UTR of *rpoS* mRNA and that CyaR expression itself is down-regulated by ArcZ through sRNA-sRNA interaction. The short form of ArcZ, but not the full-length form, can base-pair with CyaR. This ArcZ-CyaR interaction triggers degradation of CyaR by RNase E, alleviating the CyaR-mediated *rpoS* repression. These results suggest that ArcZ not only participates in *rpoS* translation as an activator, but also acts as a regulator of the reciprocally acting CyaR, maximizing its *rpoS*-activating effect.

ARTICLE HISTORY
Received 28 August 2019
Accepted 22 September 2019

KEYWORDS
Small RNAs; ArcZ; CyaR; *rpoS*; post-transcriptional regulation

Introduction

Bacteria are constantly exposed to a variety of stressful environments, experiencing specific stresses, such as temperature variation and acidic shock, and general stresses, such as entry into stationary phase and nutrient depletion [1]. Numerous targeted response mechanisms to specific stresses have been identified, but response mechanisms that function in general stresses also exist. In *Escherichia coli*, RpoS (sigma factor S) is a key regulator of general stress responses that controls approximately 500 genes [2].

RpoS expression is regulated at the levels of transcription, translation, and protein stability. The small sRNAs (sRNAs), ArcZ, DsrA and RprA, activate *rpoS* at the post-transcriptional level by directly base-pairing with *rpoS* mRNA [3,4]. These three *rpoS*-activating sRNAs stimulate *rpoS* translation by unfolding the *rpoS* mRNA 5′ UTR, exposing the translation start site of *rpoS* that is blocked by a folded stem-loop structure in the 5′ UTR [5]. ArcZ is highly expressed under aerobic conditions, but upon anaerobic stress, ArcA suppresses ArcZ, leading to down-regulation of *rpoS* expression [4]. ArcZ is processed into a short, 56-nt (nucleotide) form from the 3′ end of the 120-nt primary transcript [4,6], and the short form of ArcZ binds to the 5′ leader of *rpoS* mRNA [5]. RprA is activated by the Rcs phosphorelay, which is necessary for expression of genes needed for colonic capsule synthesis [7,8]. Activation of *rpoS* translation by RprA helps ensure properly timed expression of RpoS during biofilm maturation [9]. DsrA biosynthesis is activated in low-temperature environments [10]. OxyS is only one sRNA that has been shown to down-regulate *rpoS*, although whether it directly interacts with rpoS mRNA remains unclear [11]. Considering that RpoS is regulated in a variety of ways at the post-transcriptional level [1,12–16], the prediction is that additional *rpoS*-repressing sRNAs would be needed to cope with stresses imposed on bacteria.

Previous studies have reported that, upon overexpression, multiple sRNAs, including CyaR, down-regulate a *rpoS-lacZ* translational fusion [4]. CyaR is a cyclic AMP-activated RNA; thus, its expression is regulated by cAMP-CRP and the CpxA/R two-component system [17,18]. CyaR is sigma factor E-dependent and represses a variety of targets, including *ompX, yqaE, nadE, luxS, yobF* and *hdeD* mRNA [17–21]. Recently, Eric Masse's group analysed the targetomes of CyaR using MS2-affinity purification coupled with RNA sequencing (MAPS) technology, revealing that additional direct base-pairing target mRNAs (including *rpoS* mRNA) for CyaR may exist[21].

RNA sequencing-based experiments employing RIL-seq (RNA interaction by ligation and sequencing) or MAPS [21,22] have also identified sRNA-sRNA interaction fragments, implying that sRNA-sRNA interactions are integrated in sRNA-mediated regulatory mechanisms [21,22]. An example of regulation by sRNA-sRNA interaction is RNA 'sponges'. RNA sponges were first named for eukaryotic RNAs that contain sites capable of base-pairing with target microRNAs and minimizing microRNA-mediated mRNA repression[23]. Circular RNAs and long noncoding RNAs can also act as RNA sponges [24,25]. In bacteria, SroC sRNA, which is produced by mRNA decay from the *gltIJKL* locus encoding an amino acid ABC transporter, acts as an RNA sponge for GcvB sRNA. Because *gltIJKL* mRNA itself is a target of GcvB, the GcvB/SroC sponge system forms a feed-forward loop that regulates amino acid ABC transporters[26]. RIL-seq data[22] revealed the presence of ArcZ-CyaR interactions. However, the physiological consequences that might result from ArcZ-CyaR interactions in cells are not yet known.

CONTACT Younghoon Lee Younghoon.Lee@kaist.ac.kr Department of Chemistry, KAIST, Daejeon 34141, Korea
This article has been republished with minor changes. These changes do not impact the academic content of the article.
Supplemental Data for this article can be accessed here.

In this study, we determined (i) whether CyaR-mediated *rpoS* repression occurs through interaction of CyaR with *rpoS* mRNA, and (ii) how CyaR-ArcZ interactions contribute to *rpoS* regulation. We found that CyaR represses *rpoS* expression by binding a region immediately upstream of the ArcZ binding site in the 5′ UTR of *rpoS* mRNA. CyaR also base-pairs with the short form of ArcZ. This CyaR-ArcZ interaction triggers degradation of CyaR by RNase E, alleviating the CyaR-mediated *rpoS* repression.

Results

Repression of rpoS expression by CyaR

A previous study reported that several sRNAs down-regulate LacZ expression in a *rpoS-lacZ* translational fusion when overexpressed[27]. However, whether repression by each sRNA occurs through direct targeting of *rpoS* mRNA has remained unclear. Of these putative *rpoS*-repressing sRNAs, we focused on CyaR, first examining the *rpoS*-repressive effect of overexpressed CyaR. For this purpose, we used PM1409 strain carrying a translational *rpoS-lacZ* fusion to determine whether the *rpoS* translational repression effect occurred upon overexpression of CyaR. We found that CyaR overexpression caused a significant reduction in LacZ activity (to ~60% of controls) in *rpoS-lacZ* fusion cells (Fig 1A,B). This suggests that overexpressed CyaR represses expression of *rpoS* mRNA.

Next, we quantified levels of *rpoS-lacZ* transcripts and *rpoS* mRNA using qRT-PCR (Fig 1C,D). The levels of both *rpoS-lacZ* transcripts and *rpoS* mRNA were reduced to about 50–70% of controls by CyaR overexpression, a result consistent with the reduced level of LacZ activity (Fig 1B).

While the magnitude of CyaR repression on *rpoS* is as low as 30% ~ 40% when it is overexpressed, *rpoS*-activating sRNAs ArcZ, RprA, and DsrA increase *rpoS* expression by about 20%,

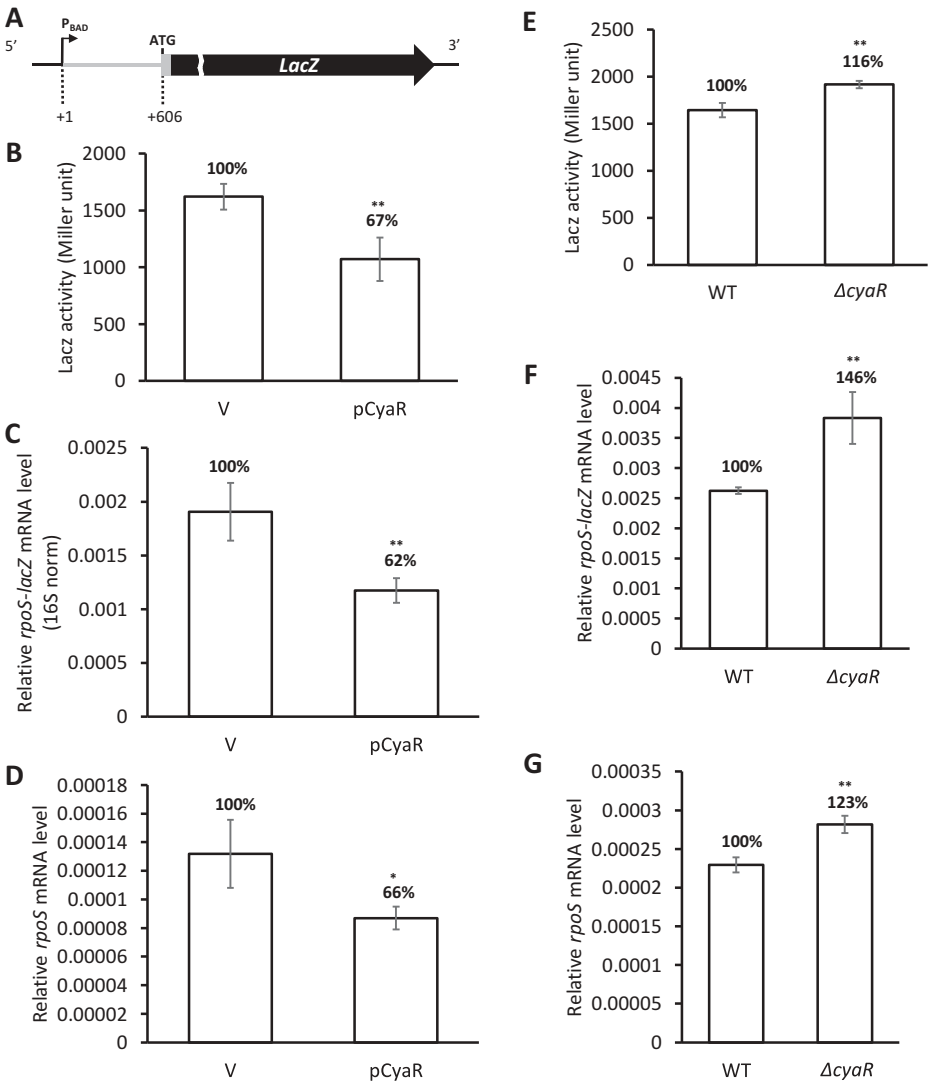

Figure 1. Repression of *rpoS* expression by CyaR. (A) Schematic presenting the *rpoS-lacZ* translational fusion. P_{BAD}, the arabinose-inducible pBAD promoter; +1, the *rpoS* transcription start site; ATG, the *rpoS* translation start codon. The sequence encoding the 5′-upstream 606 nt of the *rpoS* mRNA was fused in frame to *lacZ*. (B-D) Repression of *rpoS* by overexpression of CyaR in PM1409 (WT) cells carrying the *rpoS-lacZ* translational fusion. (B) LacZ activity, (C) *rpoS* mRNA level, and (D) *rpoS-lacZ* mRNA level were measured. mRNA levels were analysed by qRT-PCR and were normalized to *rrsA* expression. (E-G) *rpoS* activation in the absence of CyaR. (E) LacZ activity, (F) *rpoS-lacZ* mRNA level, and (G) *rpoS* mRNA level for WT and *ΔcyaR* cells were measured. The ratios of LacZ activity, and *rpoS-lacZ* and *rpoS* mRNA levels to those of WT are shown. Values are means ± SD; n = 3; **P < 0.01, *P < 0.05; ns, not significant (Student's t-test, equal variance with the control vector across expression values). pCyaR, a plasmid overexpressing CyaR; V, vector control; *ΔcyaR*, PM1409*ΔcyaR*.

70%, and 80%, respectively, under the same condition[28]. The magnitude of CyaR repression on other known targets varies from about 50% to 70% (Fig. S1). Although the CyaR repression level on *rpoS* is lower than those on other known repressible targets, it is marginally comparable to their lowest level.

Rifampicin chase experiments showed that overexpression of CyaR decreased the half-life of *rpoS* mRNA (Fig. S2). This result indicates that the repressive effect of CyaR on *rpoS* is mainly caused by degradation of *rpoS* mRNA. We examined whether RNase E, a key regulator of RNA metabolism [29–32], is involved in CyaR-mediated rpoS mRNA degradation using RNase E temperature-sensitive cells (*rne*^{ts}). To this end, we analysed *rpoS* mRNA levels following overexpression of CyaR in *rne*^{ts} cells (Fig. S3). We found that CyaR was not able to degrade *rpoS* mRNA at nonpermissive temperatures, suggesting that RNase E is crucial for CyaR-mediated *rpoS* degradation.

We also examined *rpoS* expression levels in a mutant strain lacking CyaR. In these experiments, we measured LacZ activity and *rpoS-lacZ* transcript levels generated by the *rpoS-lacZ* fusion, as well as endogenous *rpoS* mRNA levels. Compared with the WT strain, all three values were significantly increased in *ΔcyaR* cells (Fig 1E–G). This suggests that chromosomally expressed CyaR, like overexpressed CyaR, also participates in *rpoS* repression.

Structural mapping of the CyaR-rpoS mRNA interaction

To identify CyaR binding sites on the *rpoS* sequence, we performed RNA footprinting using lead acetate. For this purpose, we used the 284-nt *rpoS301* leader sequence[33]. In the presence of CyaR, we observed protection of *rpoS* mRNA from nucleotides 434 to 449 relative to the transcription start site. The protected site, which matches the pairing site for CyaR-*rpoS* mRNA interaction predicted by IntaRNA software[34], is located immediately upstream of the binding region for *rpoS*-activating sRNAs (Fig 2). Although another protected region from nucleotides 342 to 349 was observed, it probably results from the change of the secondary structure of *rpoS* mRNA by binding to CyaR because potential binding sites do not exist in this region. In addition, we also found that the region of nucleotides 449 to 460 became more vulnerable to PbAc cleavage, suggesting that this enhanced cleavage is due to the structural change of *rpoS* mRNA (Fig 2A).

To validate the CyaR-*rpoS* mRNA interaction *in vivo*, we mutated a C nucleotide at nucleotide 26 in the potential binding site of CyaR (Fig 2B). This C-to-G point mutation in CyaR suppressed CyaR-mediated *rpoS* repression (Fig 2C). A Northern blot analysis showed that the mutated CyaR was expressed at almost the same level as wild-type CyaR (Fig. S4), suggesting that the suppression of *rpoS* repression was not attributable to a decrease in the level of CyaR, but instead was caused by a loss of the interaction between CyaR and *rpoS* mRNA. To further confirm the CyaR-*rpoS* mRNA interaction, we introduced a G-to-C compensatory mutation at nucleotide 442 of *rpoS* mRNA in the *rpoS-lacZ* fusion. This G-to-C mutation also mildly suppressed *rpoS* repression by the wild type CyaR, but slightly restored the ability of the mutant CyaR to repress *rpoS* expression (Fig 2C). The G-to-C mutation at nucleotide 442 of *rpoS* mRNA disrupts a base-pair in a structural model of the full-length *rpoS* leader, which could affect the secondary structure by disrupting the 411-417/570-576 stem. We observed that LacZ activity from the *rpoSm*-lacZ fusion was increased by 20%, suggesting that the disruption of this stem causes *rpoS* activation. However, the mutant *rpoS-lacZ* fusion was activated by *rpoS*-activating sRNA ArcZ, DsrA or RprA and the increase of LacZ activity by *rpoS*-activating sRNAs in mutant cells was similar with that in wild type cells, suggesting that the *rpoS* mutation affects binding to CyaR, but binding to ArcZ, DsrA and RprA (Fig. S1A). On the other hand, the C-to-G mutation at nucleotide 26 of CyaR did not significantly affect a secondary model structure of CyaR. Furthermore, the mutant CyaR was effectively able to repress other known CyaR target genes (Fig. S1B). It seems likely, therefore, that the weak restoration effects of the mutations both in *rpoS* mRNA and CyaR is due to the *rpoS* mutation that could affect the secondary structure of the *rpoS* mRNA. Altogether, these results suggest that base-pairing between CyaR and *rpoS* is responsible for *rpoS* repression by CyaR.

Hfq dependence of CyaR-mediated rpoS repression

Since CyaR is an Hfq-dependent sRNA, we examined whether CyaR-dependent *rpoS* repression is Hfq dependent by measuring *rpoS* mRNA levels by qRT-PCR in *Δhfq* cells overexpressing CyaR and in *ΔcyaRΔhfq* double mutant cells. Interestingly, both WT and *Δhfq* cells showed similar reductions in the levels of *rpoS* mRNA upon CyaR overexpression, even though CyaR expression was decreased in the absence of Hfq (Fig 3A,C). In contrast, there was no further activation of *rpoS* by *ΔcyaR* mutation in *Δhfq* cells (Fig 3B), suggesting that endogenous CyaR cannot repress *rpoS* in *Δhfq* mutant cells. The failure of the *rpoS* repression in *Δhfq* mutant cells seems to be due to extremely low levels of CyaR (Fig 3C) in the absence of Hfq rather than the Hfq requirement for the CyaR-mediated *rpoS* repression, which is reminiscent of Hfq effects of DsrA on *rpoS* activation[28]. Therefore, it is likely that CyaR-mediated *rpoS* repression occurs in an Hfq-independent manner, despite the fact that the stability of CyaR is Hfq-dependent.

Post-transcriptional down-regulation of CyaR by ArcZ

Results of RIL-seq using Hfq[22] suggest that ArcZ and CyaR interact. We hypothesized that ArcZ and CyaR regulate each other's expression and that this regulation also contributes to *rpoS* regulation.

To test this, we examined CyaR in *arcZ*-mutant cells and ArcZ in *cyaR*-mutant cells, analysing their levels in cells at different growth time points. CyaR levels were increased at all time points examined in the absence of ArcZ (Fig 4A), whereas ArcZ levels were not significantly changed in the absence of CyaR (Fig 4B). The fold increase in CyaR levels in *arcZ*-mutant cells was largest at the time point (6 h) at which ArcZ was normally highly expressed. These results suggest that ArcZ down-regulates CyaR expression, but CyaR does not affect ArcZ expression.

We further investigated how ArcZ affects CyaR expression. To this end, we constructed a transcriptional *cyaR-lacZ* fusion strain (*cyaR*+10-*lacZ*) and examined whether ArcZ

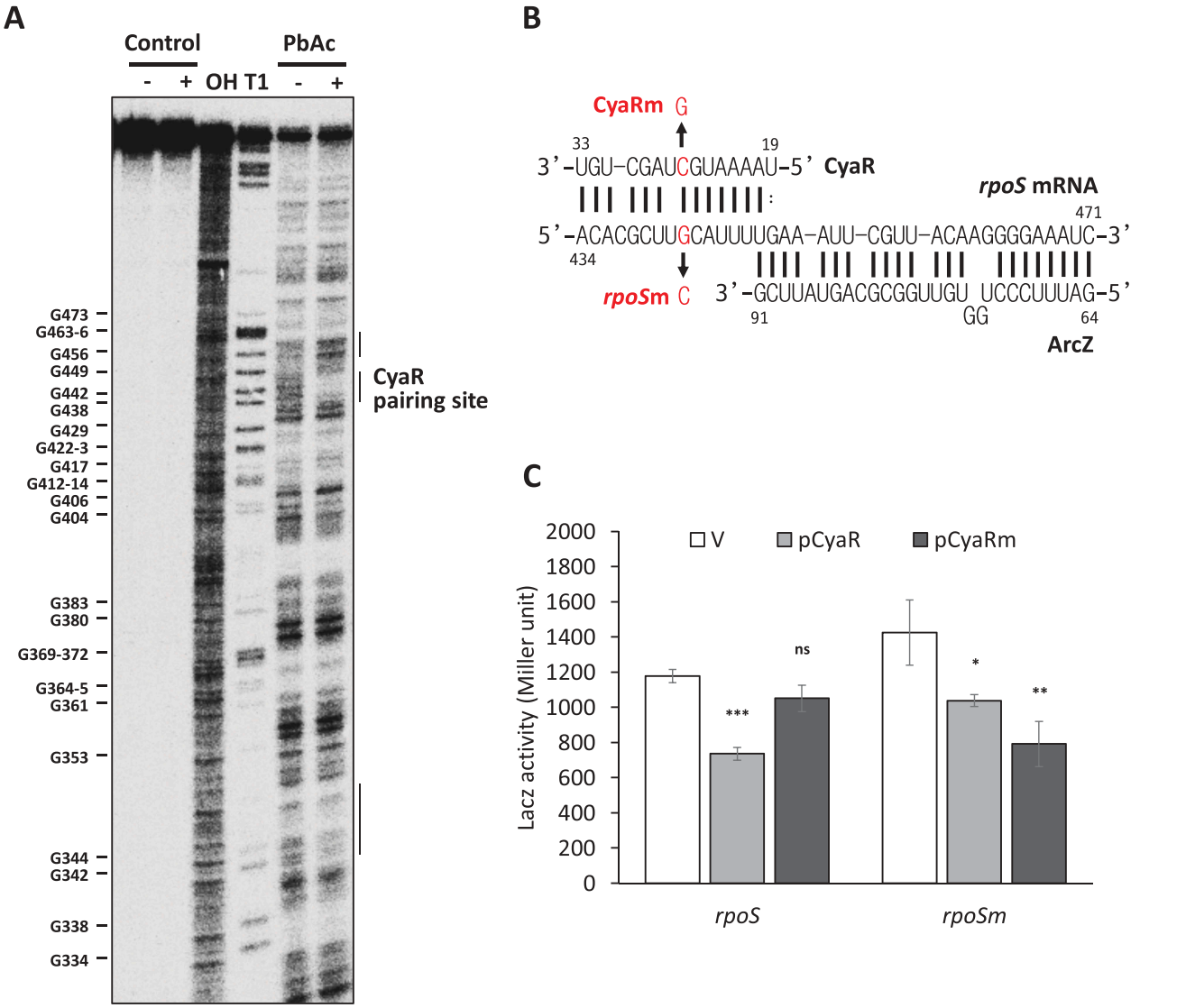

Figure 2. Probing of *rpoS* mRNA-CyaR interactions. (A) Probing of 5′ end-radiolabeled *rpoS*301 by lead acetate (PbAc) in the presence or absence of CyaR. OH, alkaline ladders; T1, RNase T1 ladders. The numbers to the left indicate G-nucleotide positions with respect to the +1 position relative to the *rpoS* transcription start site. Regions on *rpoS* mRNA that revealed significant increases or decreases in PbAc cleavage are indicated by bars on the right of the figure. (B) The base-pairing region between CyaR and *rpoS* mRNA. The C-to-G mutation at position 26 of CyaR is indicated by CyaRm, and the compensatory mutation at position +442 relative to the *rpoS* transcription start site in PM1409 is indicated by *rpoSm*. (C) Plasmids pCyaR and pCyaRm expressing CyaR and CyaRm, respectively, were introduced into strains PM1409 and PM1409m containing the compensatory mutation in *rpoS*. LacZ activity of each strain was measured and fold changes compared to the vector control (pHMB1) are shown. In (C), values are means ± SD; n = 3; ***P < 0.001, *P < 0.05 by Student's t-test. *rpoS*, PM1409; *rpoSm*, PM1409m.

overexpression affects LacZ activity (Fig 4C). LacZ activity was not changed upon ArcZ overexpression (Fig 4D), suggesting that ArcZ does not affect CyaR expression at the transcriptional level, but possibly does at the post-transcriptional level.

Degradation of CyaR through interaction with ArcZ

Since ArcZ is present as the full-length sRNA ($ArcZ_f$) and the short form ($ArcZ_s$), we examined which form of ArcZ interacts with CyaR. For this purpose, we performed RNA-RNA electrophoretic mobility shift assays (EMSAs). We found that $ArcZ_s$ bound to CyaR to form an $ArcZ_s$-CyaR complex with Kd of ~20 nM, whereas $ArcZ_f$ did not (Fig 5A–C). However, Hfq did not facilitate ArcZ-CyaR complex formation, suggesting that Hfq had little effect on ArcZ-CyaR interaction (Fig 5A,C).

To identify base-pairing regions between $ArcZ_s$ and CyaR, we probed the structures of CyaR with lead acetate in the presence of $ArcZ_s$ *in vitro*. We observed protection of CyaR nucleotides 34 to 39 in the presence of $ArcZ_s$. However, a CyaR mutant with the CA-to-GT mutation at nucleotides 36 and 37 of CyaR failed to bind to $ArcZ_s$ (Fig 5D). This protected region is in accord with the pairing site predicted by IntaRNA software (Fig 5E)[35].

To address the involvement of the ArcZ-CyaR interaction in CyaR degradation *in vivo*, we designed a two-plasmid system in which plasmids pACyaR (for CyaR expression) and pArcZ (for ArcZ expression) were introduced into the cells. Introduction of a UG-to-AC mutation at nucleotides 72 and 73 of ArcZ in pArcZ, which would disrupt interaction with CyaR, substantially increased the level of CyaR (Fig 6). This increase in CyaR levels was reduced by a compensatory CA-to-GU mutation at

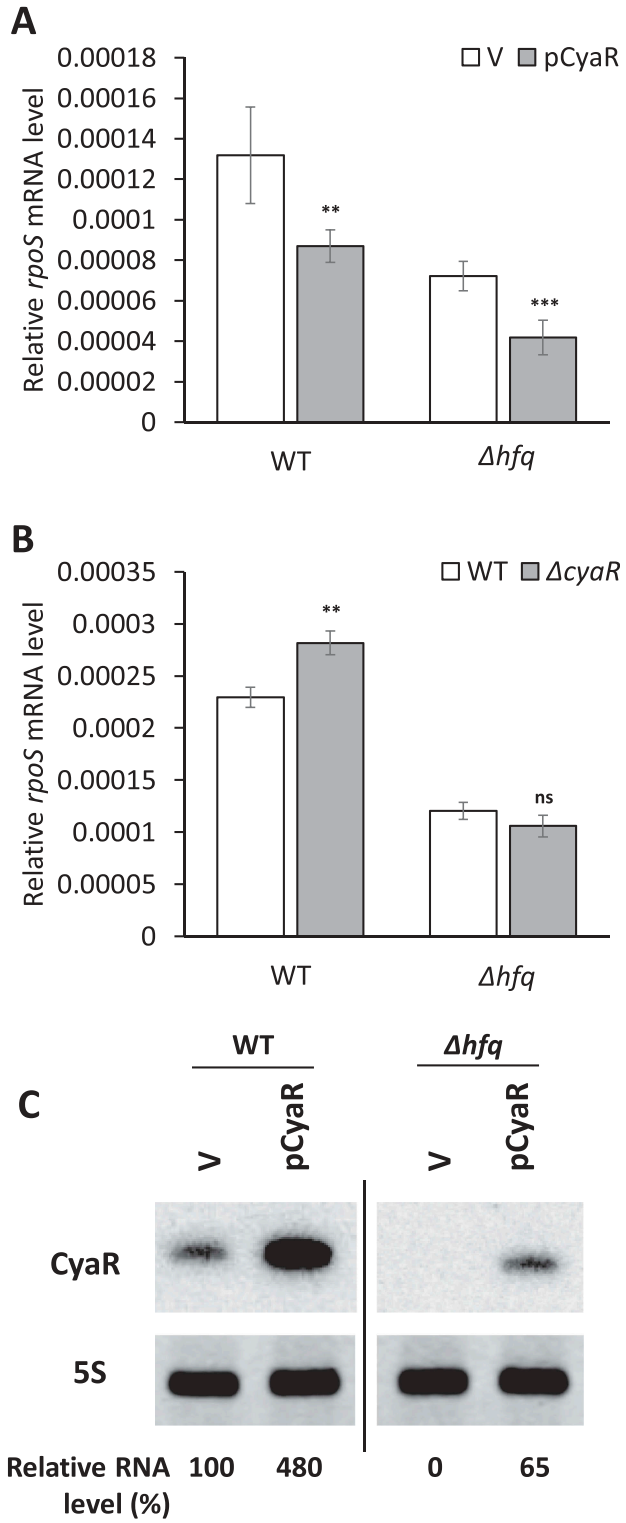

Figure 3. Hfq-independent *rpoS* repression by CyaR. The *rpoS* mRNA levels upon CyaR overexpression (A) and the *ΔcyaR* mutation (B) in *Δhfq* cells. The *rpoS* mRNA levels were measured by qRT-PCR and normalized to *rrsA* expression. Values are means ± SD; n = 3; ***P < 0.001, **P < 0.01 by Student's t-test. (C) CyaR levels were measured by Northern blot analysis. CyaR was probed with an anti-CyaR oligonucleotide; 5S rRNA is shown as a loading control. CyaR RNA quantities are expressed relative to vector controls for each strain. The spliced image from the same Northern blot membrane is shown with a dividing line inserted between spliced lanes. WT, PM1409; *Δhfq*, PM1409*Δhfq; ΔcyaRΔhfq*, PM1409*ΔcΔh*; V, vector control.

nucleotides 36 and 37 of CyaR in pACyaR, showing that the compensatory mutation restored the ability of the ArcZ mutant to reduce the level of CyaR (Fig 6).

We also performed RNA-RNA EMSA using the ArcZ mutant and the compensatory CyaR mutant. The CyaR mutant bound to the ArcZ mutant with Kd of ~200 nM, but not to the wild-type ArcZ, whereas the wild type CyaR did not bind to the ArcZ mutant (Fig. S5A-D). When probed with lead acetate, nucleotides 34 to 39 of the CyaR mutant were protected by the ArcZ mutant, but not the wild-type ArcZ (Fig. S5E).

Altogether, these results suggest that CyaR degradation by ArcZ is attributable to base-pairing between CyaR and ArcZ.

RNase E-dependent degradation of CyaR by ArcZ

Since the endoribonuclease RNase III cleaves double-stranded RNA regions in *E. coli* [32,36–38], we examined how CyaR expression is changed by ArcZ overexpression, and vice versa, in *rnc*$^-$ cells lacking RNase III. Expression of ArcZ and CyaR was not significantly changed by overexpression of CyaR and ArcZ, respectively (Fig. S6), suggesting that RNase III is not involved in ArcZ-mediated CyaR degradation.

Finally, we examined whether RNase E is involved in this process using RNase E temperature-sensitive cells (*rne*^{ts}). To this end, *rne*$^+$ and *rne*^{ts} cells were transformed with pArcZ or control vector.We analysed CyaR levels following overexpression of ArcZ and measured ArcZ levels following overexpression of CyaR (Fig 7). We observed that CyaR levels were higher with vector controls in both *rne*$^+$ and *rne*^{ts} cells at 42°C than at 30°C, suggesting CyaR expression is highly dependent on growth condition. Importantly, CyaR accumulated at 42°C upon ArcZ overexpression, whereas the level of ArcZ was not changed by CyaR overexpression. The accumulation of CyaR upon ArcZ overexpression at 42°C declined compared with vector controls. This decline in CyaR levels could be explained by the difference of the growth condition. During 15 min-IPTG induction at 30°C before shift to 42°C, CyaR in *rne*^{ts} cells could be degraded by overexpressed ArcZ, resulting in a decline in CyaR levels. Altogether, the results suggest that RNase E is required for ArcZ-mediated degradation of CyaR.

Translational regulation of rpoS by ArcZ-CyaR interaction

We examined whether ArcZ-CyaR interaction actually affects *rpoS* regulation *in vivo*. To analyse CyaR-mediated *rpoS* repression when ArcZ is lacking, we compared the increase of LacZ activity of the *rpoS-lacZ* fusion by the cyaR deletion in the *ΔarcZ* cells with that in the WT cells. We found that the cyaR deletion increased the LacZ activity more in *ΔarcZ* cells than in WT cells (Fig 8A) because *ΔarcZ* cells would lose not only *rpoS* activation but also *cyaR* repression.

We also compared *rpoS* activation upon ArcZ overexpression in WT and *ΔcyaR*cells. We found that when ArcZ is overexpressed, *ΔcyaR* cells caused less ArcZ-mediated *rpoS* activation than WT cells (Fig 8B). The less ArcZ-mediated activation would be due to the absence of ArcZ-mediated

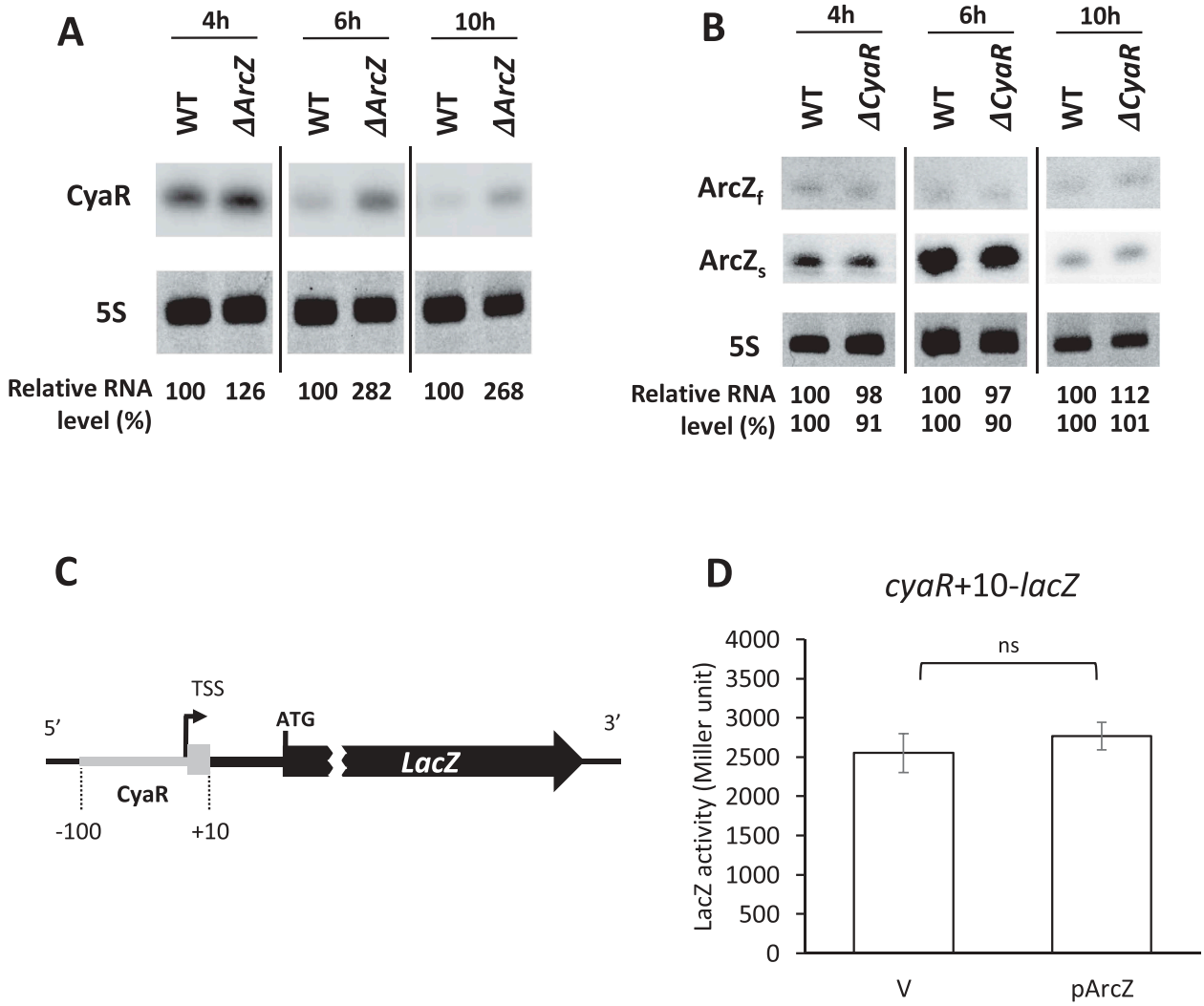

Figure 4. CyaR down-regulation by ArcZ. Overnight cultures of MG1655 (WT), *ΔarcZ*, and *ΔcyaR* cells were diluted 1:100 in LB medium and grown at 37°C. Aliquots of cells were sampled from the cultures at specific time intervals, and total cellular RNA was isolated. Cellular levels of CyaR and ArcZ were analysed by Northern blotting. (A) Cellular levels of CyaR were measured in WT and *ΔarcZ* cells during growth. CyaR was probed with an anti-CyaR oligonucleotide; 5S rRNA was detected as a loading control. (B) Cellular levels of ArcZ were measured in WT and *ΔcyaR* cells during growth. ArcZ was probed with an anti-ArcZ oligonucleotide; 5S rRNA was detected as a loading control. $ArcZ_f$, full-length form of ArcZ; $ArcZ_s$, short form of ArcZ. In (A) and (B), the spliced image from the same Northern blot membrane is shown with a dividing line inserted between spliced lanes. (C) Schematic representation of the *cyaR-lacZ* transcriptional fusion (*cyaR*+10-*lacZ*). TSS, transcription start site of CyaR. A sequence from −100 to +10 with respect to the transcription start site of CyaR was fused to *lacZ* mRNA. (D) Cells carrying the *cyaR-lacZ* transcriptional fusion were transformed with the plasmid, pArcZ, and LacZ activity was measured. Values are means ± SD; n = 3; ns, non-significant by Student's t-test; V, vector control.

cyaR repression. Altogether, the results suggest that CyaR-mediated *rpoS* repression is affected by ArcZ *in vivo*.

Discussion

In this study, we demonstrate that CyaR degrades *rpoS* mRNA by base-pairing with a region next to the ArcZ binding site in the 5′ UTR of *rpoS* mRNA, suggesting that CyaR is a *rpoS*-repressing sRNA. CyaR also interacts with the *rpoS*-activating sRNA, ArcZ. The short form of ArcZ, but not the full-length form, base-pairs with CyaR, and this ArcZ-CyaR interaction leads to degradation of CyaR and relieves *rpoS* repression by CyaR (Fig 9A).

CyaR is down-regulated by CpxR, which binds the promoter region of CyaR[39]. The CpxA/R two-component system is a complex control system that has been shown to be activated by alkaline pH shock, metal, surface adhesion, and high salt concentration[40]. In addition, genes closely involved in pH homoeostasis, such as *grcZ, focA* and *mgrB*, were predicted as targets of CyaR[21]. Here, we showed that CyaR acts as an antisense sRNA to down-regulate *rpoS* expression, which increases not only under general stress conditions, but also under acidic stress[1]. Therefore, CyaR appears to be involved in cellular regulation of more diverse stress responses.

We found that CyaR-mediated *rpoS* repression occurs in an Hfq-independent manner in the context of CysR over-expression. However, CyaR levels are very low in the absence of Hfq. Therefore, it is likely that CyaR itself can repress *rpoS* expression without Hfq, although Hfq is required for CyaR stabilization, as exemplified by *rpoS* activation by DsrA[28].

Both ArcZ and CyaR target *rpoS* mRNA while simultaneously interacting with each other. This interaction induces CyaR decay via an RNase E-dependent route (Fig 9B) and would maximize *rpoS* activation by ArcZ. Degradation of

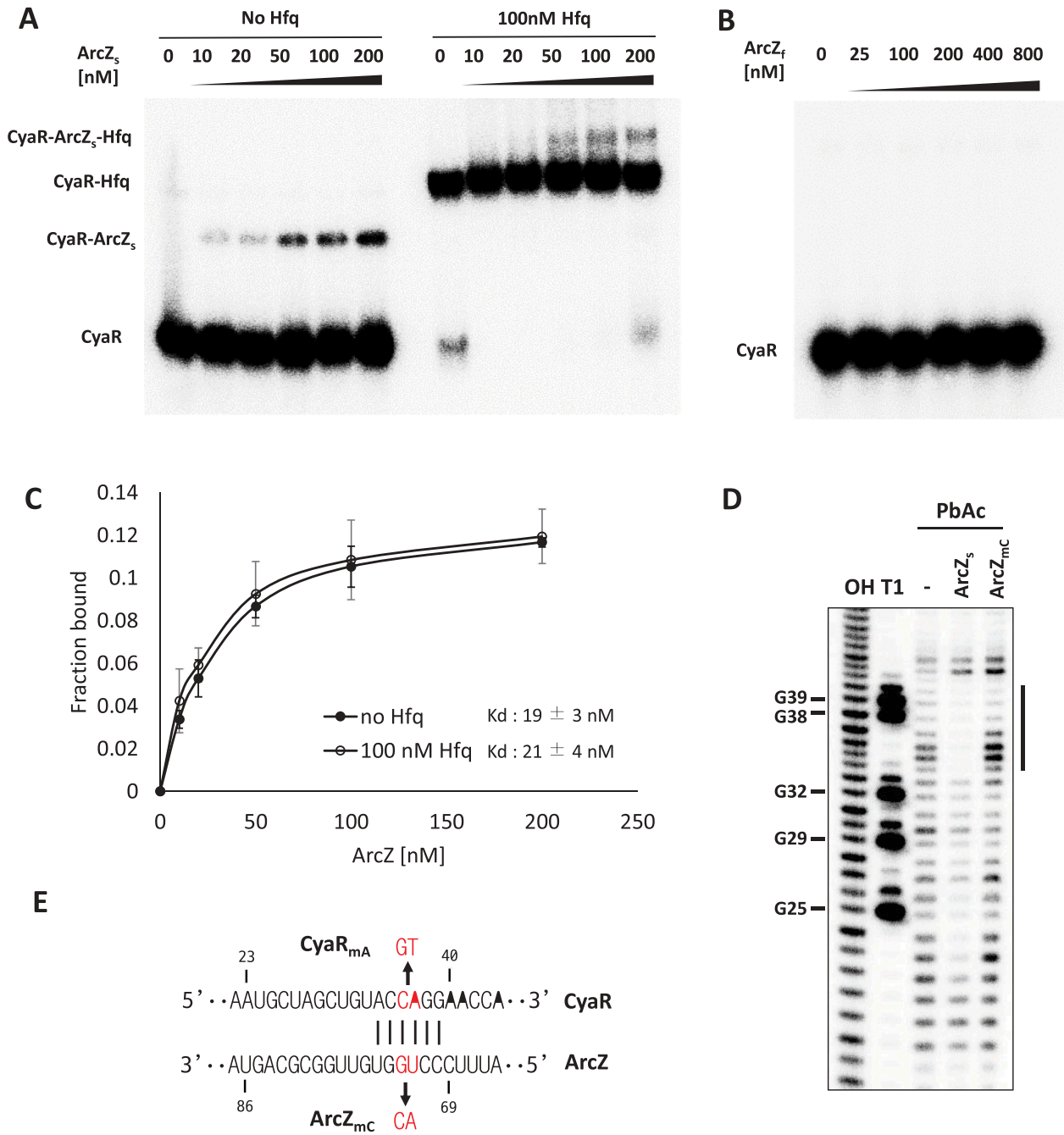

Figure 5. Interaction of CyaR with the short form of ArcZ. (A and B) EMSAs of *in vitro*-synthesized ArcZ and CyaR. ^{32}P-labelled RNA (2 nM) was incubated with the indicated concentrations of (A) $ArcZ_s$ with or without 100 nM Hfq and (B) $ArcZ_f$ without Hfq. (C) Fractions of CyaR bound to ArcZ are shown with increasing concentration of ArcZ with Hfq (open circle) or without Hfq (closed circle). Values are means ± SD; n = 3. (D) Probing of 5' ^{32}P-labelled CyaR with lead acetate (PbAc) in the presence or absence of $ArcZ_s$ or $ArcZ_{mC}$. OH, alkaline ladders; T1, RNase T1 ladders. The numbers to the left indicate sequence positions with respect to the +1 position of CyaR. A significantly protected region indicated by a bar on the right of the figure. (E) The base-pairing region between CyaR and ArcZ and the UG-to-AC mutation at positions 72 and 73 of ArcZ is indicated by $ArcZ_{mC}$ and the compensatory mutation at positions 36 and 37 of CyaR is indicated by $CyaR_{mA}$.

CyaR by ArcZ manifests in the form of ArcZ acting as a sponge for CyaR. Since SroC sRNA is known to function as a sponge for GcvB sRNA[26], and additional putative sRNA-sRNA interactions are predicted by RIL-seq data[22], it is likely that there are many other sRNA-sRNA interactions that modulate cellular metabolism in *E. coli*. Since the ArcZ-CyaR–interacting region corresponds to the *rpoS* binding sites of the respective sRNAs[4], there may be competition between sRNA-target mRNA interaction and sRNA-sRNA interaction, which could also contribute to fine-tuning of *rpoS* expression.

It was previously reported that CyaR and RprA, another *rpoS*-activating sRNA [7,8], down-regulate the same target gene, *hdeD*, through different mechanisms: CyaR induces degradation of *hdeD* mRNA, whereas two molecules of RprA block *hdeD* translation initiation[21]. Since our study showed that CyaR acts as an *rpoS*-repressing sRNA, a pair of CyaR and RprA sRNAs could also participate in fine-tuning *rpoS* expression.

ArcZ expression is suppressed by ArcA under anaerobic conditions[4], where ATP is synthesized by anaerobic

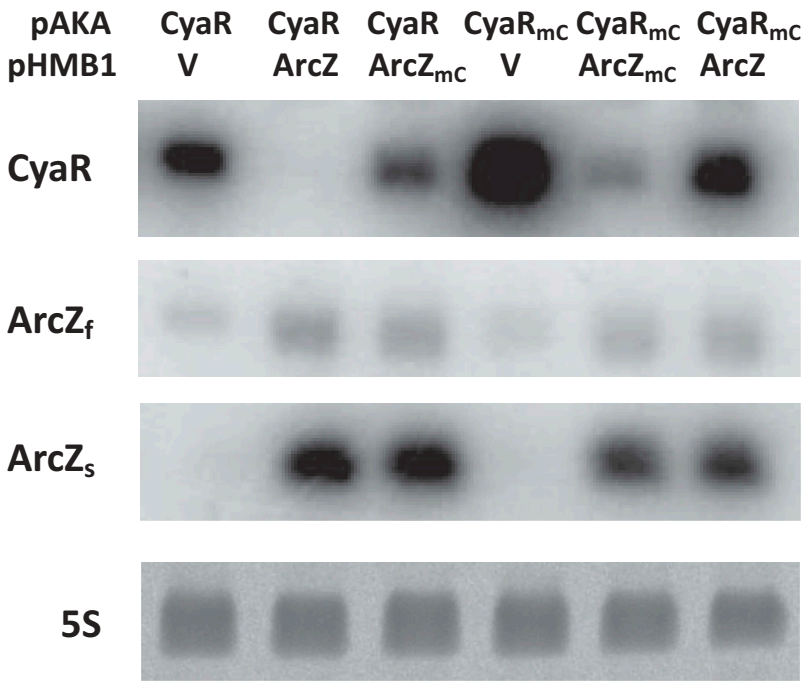

Figure 6. Degradation of CyaR by ArcZ. MG1655 cells were co-transformed with pACyaR or pACyaR$_{mA}$ and pArcZ or pArcZ$_{mC}$. IPTG was added into the culture 2 h after a 1/100 dilution of the culture (grown at 37°C) and the culture was further incubated for 2 h. Cellular levels of CyaR and ArcZ were measured by Northern blot analysis; 5S rRNA was detected as a loading control. V, vector control; CyaR, pACyaR (a derivative of pAKA); CyaR$_{mA}$, pACyaR$_{mA}$ (a derivative of pAKA); ArcZ, pArcZ (a derivative of pHMB1); ArcZ$_{mC}$, pArcZ$_{mC}$ (a derivative of pHMB1).

respiration. Anaerobic respiration can oxidize NADH to NAD^+ in the absence of oxygen, but the efficiency of this pathway is less than that of aerobic respiration. Therefore, cells may need less NAD^+ under anaerobic conditions. NAD synthetase, encoded by the CyaR target gene *nadE*, is an essential enzyme involved in both *de novo* biosynthesis and salvage of NAD^+ [41–43]. Because CyaR is the only sRNA that represses *nadE* mRNA expression at the post-transcriptional level, anaerobic down-regulation of ArcZ could increase CyaR-mediated *nadE* repression by increasing CyaR levels. CyaR regulation via ArcZ-CyaR interactions may be involved in modulating the amount of NAD synthetase during the transition from aerobic to anaerobic metabolism.

In summary, this study shows that (i) CyaR represses *rpoS* expression by directly interacting with *rpoS* mRNA, and (ii) the *rpoS*-activating sRNA ArcZ base-pairs with CyaR and degrades it in an RNase E-dependent manner. Our results suggest that ArcZ not only participates in *rpoS* translation as an activator, but also acts as a regulator of CyaR, maximizing its *rpoS*-activating effect. This coordinate regulation of *rpoS* by sRNA-sRNA interactions could contribute to the fine-tuning of *rpoS* expression to enable cells to more effectively cope with stresses.

Material and methods

Bacterial strains and plasmids

Bacterial strains and plasmids used in this study are listed in Table S1. *E. coli* strain PM1409 carrying a *rpoS-lacZ* translational fusion was a gift from Dr. S. Gottesman. PM1409*ΔcyaR*, PM1409*ΔarcZ*, PM1409*ΔcyaRΔhfq* (a *cyaR*$^-$ and *hfq*$^-$ double mutant), and PM1409*ΔcyaRΔarcZ* (a *cyaR*$^-$ and *arcZ*$^-$ double mutant) were obtained by P1 transduction [44–46] using the relevant mutant strains [47,48]. PM1409*ΔcyaRΔhfq* and PM1409*ΔcyaRΔarcZ* were constructed by removing the FRT-flanked kanamycin cassette in PM1409*ΔcyaR* using the Flp recombinase from pCP20 plasmid[49] and introducing the second *ΔarcZ* mutation and *Δhfq* mutation by P1 transduction, respectively[50]. The G-to-C mutation at position +442 relative to the *rpoS* transcription start in the *rpoS-lacZ* translational fusion was generated using scarless mutagenesis, as described previously[51]. A strain carrying the *cyaR-lacZ* transcriptional fusion (*cyaR*+10-*lacZ*) was also constructed as described previously[50]. Briefly, a *cyaR* promoter-containing fragment (−100 to +10 relative to the *cyaR* transcription start) was cloned into the *Eco*RI and *Bam*HI sites of the pRS1553 vector, and the resulting recombinant plasmid was introduced into *E. coli* strain DH408. A lysogen strain carrying the *rpoS-lacZ* transcriptional fusion was constructed using λRS468. RNA expression vectors pHMB1 and pAKA, derived from pBR322 and p15A, respectively, were used to generate CyaR- or ArcZ-expressing plasmids, as described previously[52]. The oligonucleotides employed are listed in Table S2.

LacZ activity assay

Three colonies for each strain were cultured overnight in LB medium, then overnight cultures were diluted 1:100 and grown in fresh medium. Where necessary, ampicillin (100 μg/ml) or both ampicillin (100 μg/ml) and tetracycline (10 μg/ml) were added to the medium to maintain plasmid-bearing cells. For *cyaR-lacZ* transcriptional fusion-containing cells, 0.1 mM IPTG (isopropyl β-D-1-thiogalactopyranoside)

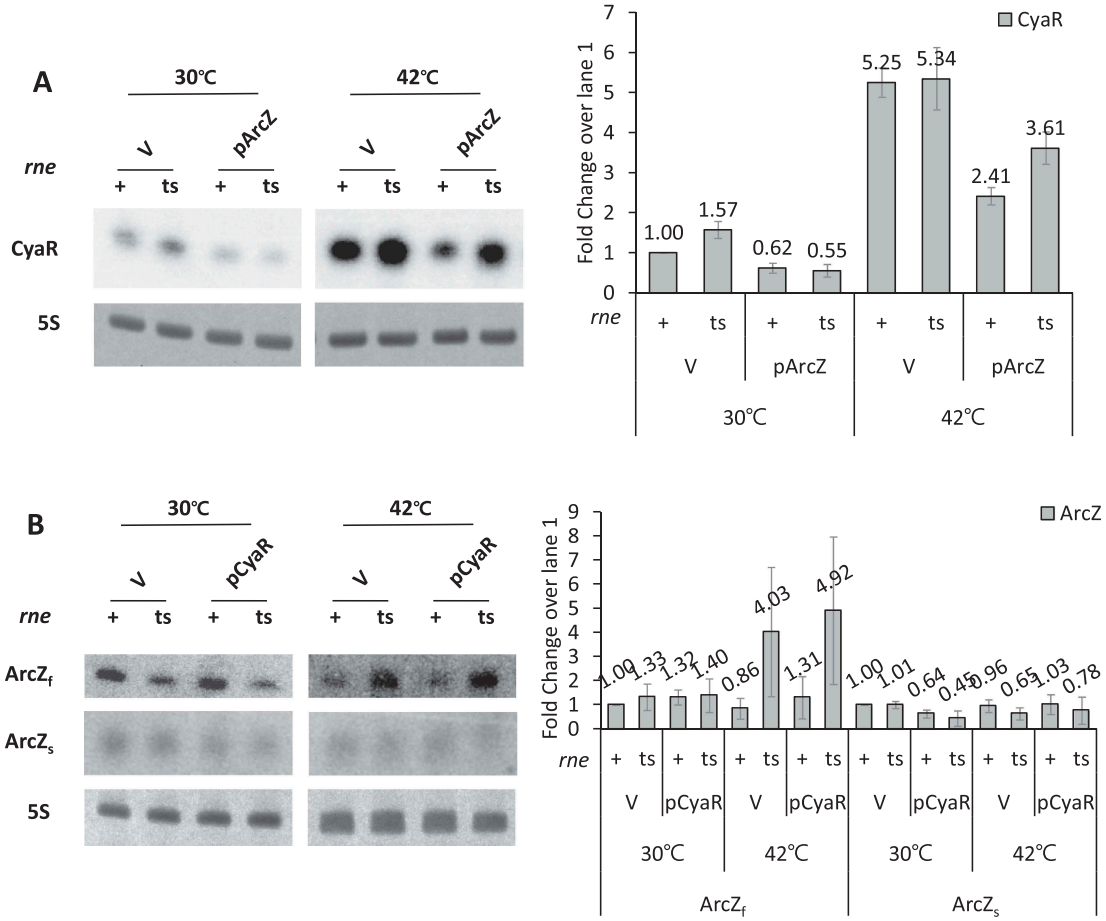

Figure 7. RNase E-dependent degradation of CyaR by ArcZ. (A) MCE+ (*rne*$^{+}$) and MCE- (*rne*^{ts}) cells were transformed with pArcZ. IPTG was added 4 h after a 1/100 dilution of culture (grown at 30°C), and the culture was further incubated for 15 min. Cultures were heat-shocked for 15 min at 42°C or incubated for 15 min at 30°C. Total cellular RNA was prepared from the cultures, and cellular levels of CyaR were measured by Northern blot analysis using an anti-CyaR oligonucleotide probe; 5S rRNA was detected as a loading control. (B) The *rne*$^{+}$ and *rne*^{ts} cells were transformed with pCyaR. ArcZ levels were analysed as described in (A). Bar graphs show fold changes of ArcZ transcripts ($ArcZ_f$ and $ArcZ_s$) compared with vector controls at 30°C.

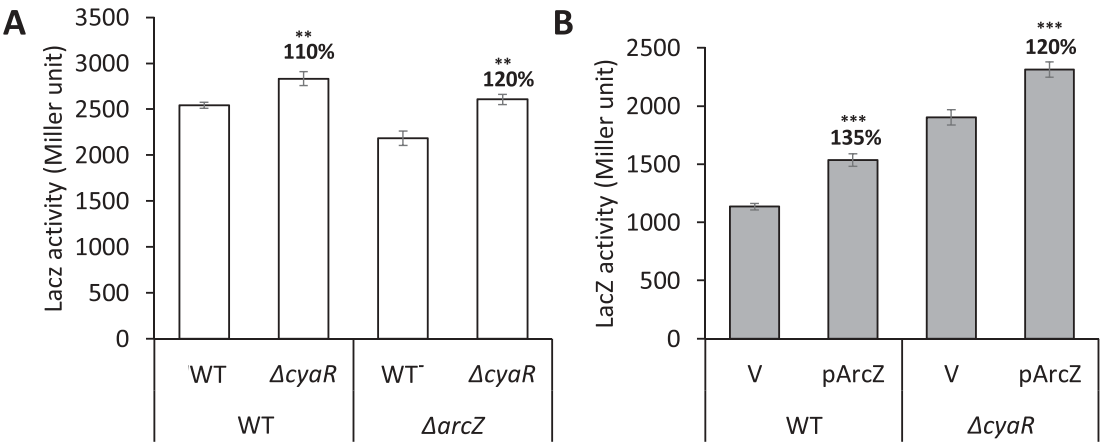

Figure 8. Translational regulation of *rpoS* by CyaR-ArcZ interaction *in vivo*. (A) Overnight cultures of PM1409 (WT), *ΔcyaR, ΔarcZ*, or *ΔcyaRΔarcZ* were diluted 1:100 in LB medium. Cells were grown at 37°C for 4 h and induced with 0.002% arabinose. The culture was incubated further for 2 h and LacZ activity was measured. (B) WT or *ΔcyaR* were transformed with pArcZ. The overnight cultures were diluted 1:100 and grown at 37°C. Arabinose of 0.002% and 0.1 mM IPTG were added at 2 h and 3.5 h after 1/100 dilution, respectively, and the culture was incubated further for 0.5 h. LacZ activity was measured. Values are means ± SD; n = 3; ***P < 0.001, **P < 0.01, by student's t-test. *ΔcyaR*, PM1409*ΔcyaR; ΔarcZ*, PM1409*ΔarcZ; ΔcyaRΔarcZ*, PM1409*ΔcΔa*.

was added 3.5 h after diluting, and the culture was further incubated for 0.5 h. For *rpoS-lacZ* translational fusion-containing cells, 0.002% arabinose and IPTG were added at 2 h and 3.5 h, respectively, and the culture was incubated for

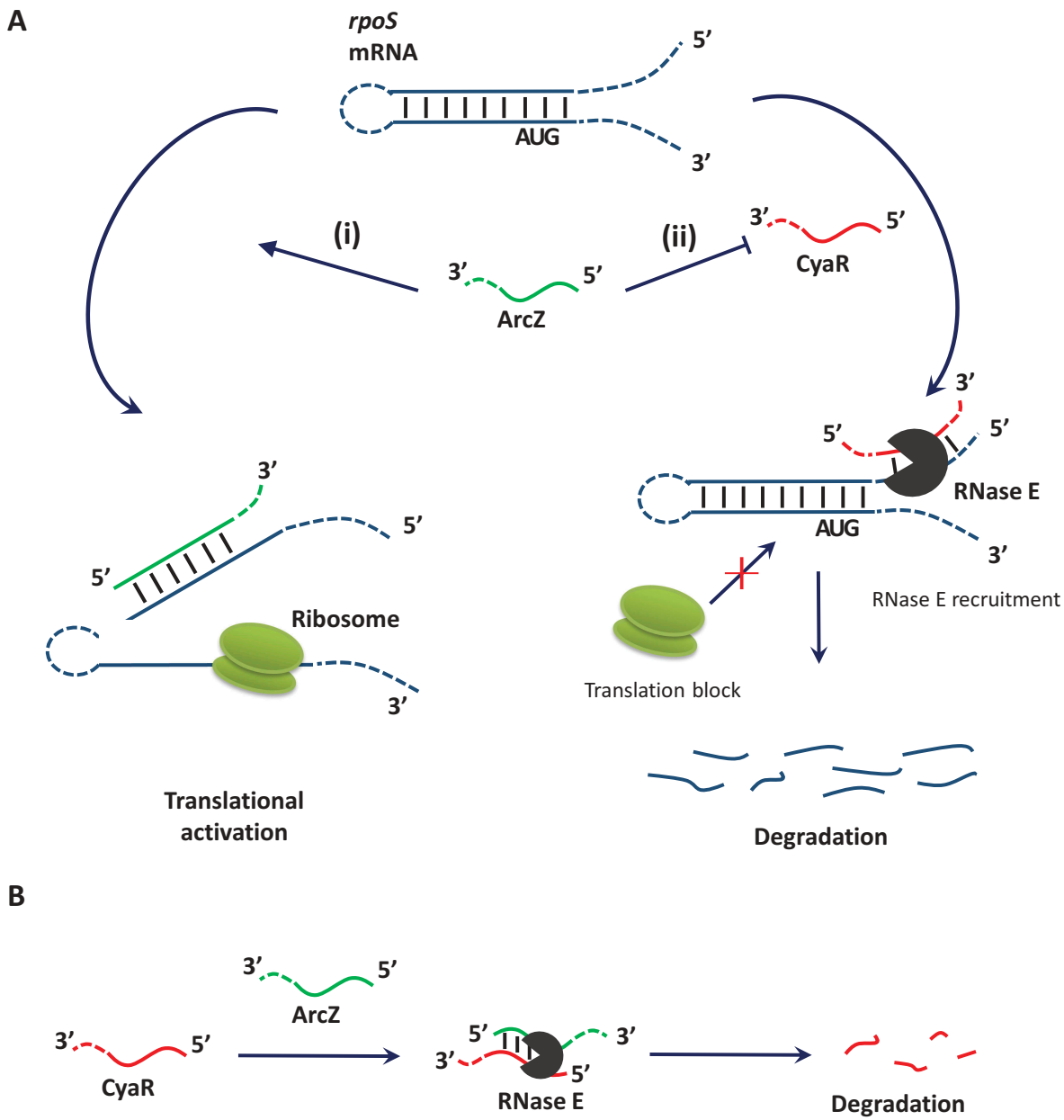

Figure 9. A model for coordinate regulation of *rpoS* by ArcZ-CyaR interactions. (A) ArcZ up-regulates *rpoS* expression by different mechanisms: (i) base-pairing with the 5′ UTR of *rpoS* to open up an inhibitory hairpin; and (ii) repression of CyaR-dependent *rpoS* degradation. (B) Mechanism of CyaR regulation by ArcZ. ArcZ base-pairs with CyaR and degrades CyaR through RNase E.

an additional 0.5 h. LacZ activity was assayed as described previously[53]. At least three independent measurements were made for each strain.

Northern blot analysis

Cells were grown as described in the LacZ activity assay section, above. Total cellular RNA was extracted from the culture using acidic hot phenol, as described previously[54]. Total RNA (10 μg) was fractionated on a 7 M urea, 5% polyacrylamide gel, and electrotransferred onto a Hybond-XL membrane (Amersham Biosciences), as previously described[55]. The membrane was hybridized with ^{32}P-labelled DNA probes in Rapid-Hyb buffer (Amersham Biosciences) according to the manufacturer's instructions. Hybridization signals were analysed using an FLA7000 Image Analyser (Fuji). The utilized probes are listed in Table S2.

RNA stability assay

Three colonies for each strain were cultured in LB medium containing ampicillin (100 μg/ml) at 37°C, and the overnight culture was diluted to 1:100 and cultured with the fresh medium. Arabinose (0.002%) and 0.1 mM IPTG were added at 2 h and 3 h 50 min, respectively, and the culture was incubated further for 10 min. Transcription were halted by the addition of rifampicin (a final concentration of 500 μg/ml) and aliquots of the culture were sampled at intervals. Total

cellular RNAs were prepared and subjected to Northern blot analysis or qRT-PCR.

In vitro transcription

CyaR, *rpoS301* carrying the 284-nt *rpoS* leader sequence[33], the full-length form of ArcZ, and the short form of ArcZ were prepared by *in vitro* transcription. DNA templates were obtained by polymerase chain reaction (PCR) using appropriate primer pairs (Table S2), and *in vitro* transcription was carried out using T7 RNA polymerase (Promega). RNA transcripts were gel-purified, as described[53].

Quantitative reverse transcription-PCR (qRT-PCR)

Total cellular RNA was treated to remove any DNA contaminants using a TURBO DNA-*free* Kit (Ambion). cDNA was synthesized from DNase-treated RNA using a SuPrimeScript RT-PCR premix (Genet Bio) and amplified with SuPrimeScript qRT-PCR Premix (Genet Bio) on a Bioneer Exicycle 96 Real-Time Quantitative Thermal Block (Bioneer). Primer pairs specific to the *lacZ* ORF, *rpoS* ORF, or *rrsA* mRNA were used for qRT-PCR (Table S2).

Electrophoretic mobility shift assay (EMSA)

The Hfq protein was purified as described previously[56]. All purified RNAs were renatured by heating for 1 min at 95°C and slowly cooling to 25°C. CyaR (2 nM), labelled at the 5′ end with ^{32}P, was incubated with increasing amounts of ArcZ transcripts for 20 min at 25°C in 20 µl TMN buffer [100 mM Tris–acetate pH 7.6, 500 mM NaOAc, 25 mM $Mg(OAc)_2$][57] in the presence or absence of 0.1 µM Hfq. The reaction was stopped by adding 1/6th volume of non-denaturing loading buffer (0.025% xylene cyanol, 2% glycerol, 1X TBE), after which reaction mixtures were analysed on 5% non-denaturing polyacrylamide gels at 4°C.

RNA footprinting

All purified RNAs were renatured as described in the EMSA section, above. ^{32}P-labelled *rpoS301* and CyaR (20 nM each) were incubated with 500 nM CyaR in 10 µl annealing buffer (250 mM Tris-HCl pH7.5, 1.25 M NaCl, 1.25 M KCl)[58] and 500 nM ArcZ in 10 µl TMN buffer, respectively, for 20 min at 25°C. Then, 20 mM lead acetate was added, followed by incubation at 25°C for 15 min in 20 µl of 1x structure buffer (Ambion). Reactions were stopped by adding 1 µl of 0.5 M EDTA and 20 µl of 2x RNA dye. The same ^{32}P-labelled *rpoS301* and CyaR were separately incubated for 5 min at 95°C in alkaline buffer or 15 min at 25°C with ribonuclease T1 (0.1 U; Ambion) to generate alkaline (OH) and T1 ladders, respectively. Cleavage products were heated at 95°C for 3 min and analysed on a 4% (for *rpoS301*) or 7% (for CyaR) polyacrylamide-9 M urea sequencing gel.

Acknowledgments

This study was supported by National Research Foundation of Korea (NRF) Grants from the Korean government (MSIT) (2019R1H1A2039730) and by KAIST. The authors would like to thank Dr. S. Gottesman for providing strain PM1409 and Prof. S. A. Woodson for providing a vector expressing Hfq.

Disclosure statement

No potential conflict of interest was reported by the authors.

Funding

This work was supported by the KAIST; National Research Foundation of Korea (NRF) Grants [2019R1H1A2039730].

ORCID

Younghoon Lee http://orcid.org/0000-0002-3841-719X

References

[1] Battesti A, Majdalani N, Gottesman S. The RpoS-mediated general stress response in escherichia coli. Annu Rev Microbiol. 2010;65:189–213.
[2] Hirsch M, Elliott T. Stationary-phase regulation of RpoS translation in Escherichia coli. J Bacteriol. 2005;187(21):7204–7213.
[3] McCullen CA, Benhammou JN, Majdalani N, et al. Mechanism of positive regulation by DsrA and RprA small noncoding RNAs: pairing increases translation and protects rpoS mRNA from degradation. J Bacteriol. [Internet] 2010;192:5559–5571. [cited 2014 Feb 27]. Available from: http://www.pubmedcentral.nih.gov/articlerender.fcgi?artid=2953674&tool=pmcentrez&rendertype=abstract
[4] Mandin P, Gottesman S. Integrating anaerobic/aerobic sensing and the general stress response through the ArcZ small RNA. Embo J. [Internet] 2010; 29:3094–3107. [cited 2014 Feb 26]. Available from: http://www.pubmedcentral.nih.gov/articlerender.fcgi?artid=2944060&tool=pmcentrez&rendertype=abstract
[5] Soper T, Mandin P, Majdalani N, et al. Positive regulation by small RNAs and the role of Hfq. Proc Natl Acad Sci U S A. [Internet] 2010; 107:9602–9607. [cited 2014 Feb 12]. Available from: http://www.pubmedcentral.nih.gov/articlerender.fcgi?artid=2906882&tool=pmcentrez&rendertype=abstract
[6] Papenfort K, Said N, Welsink T, et al. Specific and pleiotropic patterns of mRNA regulation by ArcZ, a conserved, Hfq-aependent small RNA. Mol Microbiol. 2009;74:139–158.
[7] Majdalani N, Hernandez D, Gottesman S. Regulation and mode of action of the second small RNA activator of RpoS translation, RprA. Mol Microbiol. 2002;46(3):813–826.
[8] Mika F, Busse S, Possling A, et al. Targeting of csgD by the small regulatory RNA RprA links stationary phase, biofilm formation and cell envelope stress in Escherichia coli. Mol Microbiol. 2012;84(1):51–65.
[9] Ferrières L, Thompson A, Clarke DJ. Elevated levels of σS inhibit biofilm formation in Escherichia coli: A role for the Rcs phosphorelay. Microbiology. 2009;155(11):3544–3553.
[10] Sledjeski DD, Gupta A, Gottesman S. The small RNA, DsrA, is essential for the low temperature expression of RpoS during exponential growth in Escherichia coli. Embo J. [Internet] 1996; 15:3993–4000. Available from: http://www.ncbi.nlm.nih.gov/pmc/articles/PMC452119/
[11] Zhang A, Altuvia S, Tiwari A, et al. The OxyS regulatory RNA represses rpoS translation and binds the Hfq (HF-I) protein. Embo J. 1998;17(20):6061–6068.

[12] Loewen PC, Hu B, Strutinsky J, et al. Regulation in the rpoS regulon of Escherichia coli. Can J Microbiol. 2011;44(8):707–717.
[13] Gottesman S. The small RNA regulators of Escherichia coli: roles and mechanisms*. Annu Rev Microbiol. 2004;58:303–328.
[14] Dong T, Schellhorn HE. Control of RpoS in global gene expression of Escherichia coli in minimal media. Mol Genet Genomics. 2009;281(1):19–33.
[15] Patten CL, Kirchhof MG, Schertzberg MR, et al. Microarray analysis of RpoS-mediated gene expression in Escherichia coli K-12. Mol Genet Genomics. 2004;272(5):580–591.
[16] Sedlyarova N, Shamovsky I, Bharati BK, et al. sRNA-mediated control of transcription termination in E. Coli Cell. 2016;167:111–121.e13.
[17] De Lay N, Gottesman S. The crp-activated small noncoding regulatory RNA CyaR (RyeE) links nutritional status to group behavior. J Bacteriol. 2009;191:461–476.
[18] Johansen J, Eriksen M, Kallipolitis B, et al. Down-regulation of outer membrane proteins by noncoding RNAs: unraveling the cAMP-CRP- and σE-dependent CyaR-ompX regulatory case. J Mol Biol. 2008;383:1–9.
[19] Papenfort K, Pfeiffer V, Lucchini S, et al. Systematic deletion of Salmonella small RNA genes identifies CyaR, a conserved CRP-dependent riboregulator of OmpX synthesis. Mol Microbiol. 2008;68:890–906.
[20] Wright PR, Richter AS, Papenfort K, et al. Comparative genomics boosts target prediction for bacterial small RNAs. Proc Natl Acad Sci. 2013;110(37):E3487–96.
[21] Lalaouna D, Prévost K, Laliberté G, et al. Contrasting silencing mechanisms of the same target mRNA by two regulatory RNAs in Escherichia coli. Nucleic Acids Res. 2018;46:2600–2612.
[22] Melamed S, Peer A, Faigenbaum-Romm R, et al. Global mapping of small RNA-target interactions in bacteria. Mol Cell. 2016;63:884–897. Internet.
[23] Ebert MS, Neilson JR, Sharp PA. MicroRNA sponges: competitive inhibitors of small RNAs in mammalian cells. Nat Methods. 2007;4(9):721.
[24] Salzman J. Circular RNA expression: its potential regulation and function. Trends Genet. 2016;32(5):309–316.
[25] Du Z, Sun T, Hacisuleyman E, Fei T, Wang X, Brown M, Rinn JL, Lee MG-S, Chen Y, Kantoff PW, et al. Integrative analyses reveal a long noncoding RNA-mediated sponge regulatory network in prostate cancer. Nature Communications [Internet] 2016;7:10982. Available from: https://doi.org/10.1038/ncomms10982
[26] Miyakoshi M, Chao Y, Vogel J. Cross talk between ABC transporter mRNAs via a target mRNA-derived sponge of the GcvB small RNA. Embo J. 2015;34:1478–1492.
[27] Moon K, Gottesman S. Competition among Hfq-binding small RNAs in Escherichia coli. Mol Microbiol. 2011;82:1545–1562.
[28] Kim W, Choi JS, Kim D, et al. Mechanisms for Hfq-independent activation of rpoS by DsrA, a small RNA, in Escherichia coli. Mol Cells. 2019;42:1–15.
[29] Mackie GA, RNase E. At the interface of bacterial RNA processing and decay. Nat Rev Microbiol. 2013;11:45–57.
[30] Carpousis AJ. The RNA degradosome of escherichia coli : an mRNA-degrading machine assembled on RNase E. Annu Rev Microbiol. 2007;61:71–87.
[31] Morita T, Maki K, Aiba H. RNase E-based ribonucleoprotein complexes: mechanical basis of mRNA destabilization mediated by bacterial noncoding RNAs. Genes Dev. 2005;19:2176–2186.
[32] Massé E, Escorcia FE, Gottesman S. Coupled degradation of a small regulatory RNA and its mRNA targets in Escherichia coli. Genes Dev. 2003;17:2374–2383.
[33] Peng Y, Soper TJ, Woodson SA. Positional effects of AAN Motifs in rpoS regulation by sRNAs and Hfq. J Mol Biol. [Internet] 2013; 426:275–285. [cited 2014 Mar 6]. Available from: http://www.ncbi.nlm.nih.gov/pubmed/24051417
[34] Sorescu DA, Mann M, Kleinkauf R, et al. CopraRNA and IntaRNA: predicting small RNA targets, networks and interaction domains. Nucleic Acids Res. 2014;42:W119–23. Internet.
[35] Sorescu DA, Mann M, Kleinkauf R, et al. CopraRNA and IntaRNA: predicting small RNA targets, networks and interaction domains. Nucleic Acids Res. 2014;42:W119–23.
[36] Lybecker M, Zimmermann B, Bilusic I, et al. The double-stranded transcriptome of Escherichia coli. Proc Natl Acad Sci. 2014;111 (8):3134–3139.
[37] Court DL, Gan J, Liang Y-H, et al. RNase II: genetics and function; structure and mechanism. Annu Rev Genet. 2013;47:405–431.
[38] Nicholson AW. Ribonuclease III mechanisms of double-stranded RNA cleavage. Wiley Interdiscip Rev RNA. 2014;5(1):31–48.
[39] Vogt SL, Evans AD, Guest RL, et al. The Cpx envelope stress response regulates and is regulated by small noncoding RNAs. J Bacteriol. 2014;196:4229–4238.
[40] Hunke S, Keller R, Müller VS. Signal integration by the Cpx-envelope stress system. FEMS Microbiol Lett. 2012;326(1):12–22.
[41] Hughes KT, Olivera BM, Roth JR. Structural gene for NAD synthetase in Salmonella typhimurium. J Bacteriol. 1988;170:2113–2120.
[42] Schneider BL, Reitzer LJ. Salmonella typhimurium nit is nadE: defective nitrogen utilization and ammonia-dependent NAD synthetase. J Bacteriol. 1998;180.
[43] Willison JC, Tissot G. The Escherichia coli efg gene and the Rhodobacter capsulatus adgA gene code for NH3-dependent NAD synthetase. J Bacteriol. 1994;176:3400–3402.
[44] Macdonald DW, Buesching CD, Stopka P, et al. Encounters between two sympatric carnivores: red foxes (Vulpes vulpes) and European badgers (Meles meles). J Zool. 2004;263:385–392.
[45] Moore SD. Assembling new escherichia coli strains by transduction using phage P1. Methods Mol Biol. 2011;765:155–169.
[46] Thomason LC, Costantino N, Court DL. E. coli genome manipulation by P1 transduction [Internet]. Curr Protoc Mol Biol. 2007;79(1):1–7.
[47] Bak G, Lee J, Suk S, et al. Identification of novel sRNAs involved in biofilm formation, motility, and fimbriae formation in Escherichia coli. Sci Rep. 2015;5:15287. Internet.
[48] Bak G, Han K, Kim D, et al. Roles of rpoS- activating small RNAs in pathways leading to acid resistance of Escherichia coli. Microbiologyopen. 2014;3:15–28.
[49] Cherepanov PP, Wackernagel W. Gene disruption in Escherichia coli: tcR and KmR cassettes with the option of Flp-catalyzed excision of the antibiotic-resistance determinant. Gene. [Internet] 1995; 158:9–14. Available from: http://www.sciencedirect.com/science/article/pii/037811199500193A
[50] Müller-Hill B. Experiments with gene fusions. Trends Genet. 1985;1:61.
[51] Blank K, Hensel M, Gerlach RG. Rapid and highly efficient method for scarless mutagenesis within the salmonella enterica chromosome. PLoS One. 2011 cited 2019 Apr 3;6:e15763. Internet
[52] Han K, Kim KS, Bak G, et al. Recognition and discrimination of target mRNAs by Sib RNAs, a cis-encoded sRNA family. Nucleic Acids Res. 2010;38:5851–5866.
[53] Xiangyang ZHB. Control of the Escherichia coli rrnB P1 promoter strength by ppGpp. J Biol Chem. 1995;270:11181–11189.
[54] Kim S, Kim H, Park I, et al. Mutational analysis of RNA structures and sequences postulated to affect 3′ processing of M1 RNA, the RNA component of Escherichia coli RNase P. J Biol Chem. 1996;271:19330–19337.
[55] Park H, Bak G, Kim SC, et al. Exploring sRNA-mediated gene silencing mechanisms using artificial small RNAs derived from a natural RNA scaffold in Escherichia coli. Nucleic Acids Res. [Internet] 2013; 41:3787–3804. [cited 2014 Feb 20]. Available from: http://nar.oxfordjournals.org/cgi/content/long/41/6/3787
[56] Santiago-Frangos A, Kavita K, Schu DJ, et al. C-terminal domain of the RNA chaperone Hfq drives sRNA competition and release of target RNA. Proc Natl Acad Sci. [Internet] 2016; 113:E6089–96. Available from: http://www.pnas.org/lookup/doi/10.1073/pnas.1613053113
[57] Han K, Kim K, Bak G, et al. Recognition and discrimination of target mRNAs by Sib RNAs, a cis -encoded sRNA family. Nucleic Acids Res. 2010;38:5851–5866.
[58] Soper TJ, Woodson SA. The rpoS mRNA leader recruits Hfq to facilitate annealing with DsrA sRNA. RNA. [Internet] 2008; 14:1907–1917. Available from: http://www.ncbi.nlm.nih.gov/pmc/articles/PMC2525945/